INFLUENCE OF EL NIÑO ON PARAMETERS
OF THE MIDDLE AND UPPER ATMOSPHERE OVER EASTERN SIBERIA
ACCORDING TO REANALYSIS AND MODEL DATA IN WINTER

A.N. Vyatkin
Institute of Solar-Terrestrial Physics SB RAS,
Irkutsk, Russia, aptemzm1997@gmail.com

O.S. Zorkaltseva
Institute of Solar-Terrestrial Physics SB RAS,
Irkutsk, Russia, meteorologist-ka@yandex.ru

V.I. Mordvinov
Institute of Solar-Terrestrial Physics SB RAS,
Irkutsk, Russia, v_mordv@iszf.irk.ru

Abstract. One of the most important climate-forming phenomena in the ocean—atmosphere system is the El Niño Southern Oscillation (ENSO) events, which manifest themselves with varying intensity in almost all regions of the globe. The central regions of Eurasia are farthest from the tropics of the Pacific Ocean, the regions where ENSO originates. There are different points of view regarding the nature of the ENSO effect on these regions. In the presented work, the influence of ENSO on the upper atmosphere of the Northern Hemisphere and, in particular, on the upper atmosphere of Eastern Siberia is estimated using model calculations and reanalysis data. The results of the analysis show that the large-scale structures of the atmospheric response to the ENSO events in the Northern Hemisphere are similar according to modeling and reanalysis, yet the regions of Eastern Siberia are on the periphery of the main signal and there are significant differences in estimated effects from one case of El Niño and La Niña to another. In January, ENSO has the greatest impact on the middle atmosphere of the polar regions of the Northern Hemisphere. Over Eurasia and Eastern Siberia, the atmospheric response to the ENSO events turned out to be weak or absent.

Keywords: El Niño Southern Oscillation, mesosphere — lower thermosphere, planetary waves, MUAM.

INTRODUCTION

The El Niño Southern Oscillation (ENSO) is the interaction between the ocean and the atmosphere in the Equatorial Pacific. El Niño events exhibit an increase in the sea surface temperature in the Central Pacific, a large number of clouds over the Central and Eastern Pacific, and Walker circulation anomalies [Wang et al., 2021]. ENSO has the greatest impact on the troposphere of low latitudes; however, it affects the atmospheric circulation almost all over the globe and in all atmospheric layers. ENSO, for example, causes the equatorial stratosphere to cool and the temperature gradient between the low-latitude atmosphere and the polar vortex to decrease, weakening the latter. In the mean, the polar stratospheric vortex during El Niño is weaker than during La Niña [Lu et al., 2011]. This indicates that the high-latitude winter stratosphere is, on average, warmer during El Niño, but the mesosphere is colder, which is confirmed by satellite data and model experiments [Garcia-Herrera et al., 2006; Lu et al., 2011; Li et al., 2013]. It is believed that El Niño leads to an increased probability of sudden stratospheric warming (SSW) events [Taguchi, Hartmann, 2006; Domeisen et al., 2019]. There is evidence that El Niño manifests itself in the upper atmosphere. For instance, in [Jacobi, Kürschner, 2002; Jacobi et al., 2017], a correlation has been found between the ENSO index (Niño3) and the zonal wind at an altitude of 90 km above Germany. Comparing the time series of the ENSO index and the wind in the mesosphere — lower thermosphere (MLT) has shown that in January–February zonal winds correlate with ENSO, with a delay of about one month. The most significant correlations occurred at ~90 km and weakened with decreasing altitude.

Presumably, an important factor determining the dependence of the upper atmosphere on El Niño is wave activity in the atmosphere. As shown in [Ermakova et al., 2022], El Niño of different types features different wave activity levels, variations in the temperature of the polar stratosphere and in the zonal wind velocity, which, in turn, can affect the time of polar vortex destruction and the beginning of spring restructuring in the stratosphere. This assumption does not contradict classical concepts according to which the ENSO-induced changes in atmospheric parameters in the upper troposphere affect the structure and width of the stratospheric waveguide having an effect on vertical propagation of planetary waves from the troposphere, which causes variability in stratospheric dynamic processes in the extratropical region [Richter et al., 2011; Lubis et al., 2016].

A premise of this study was the works [Mikhalev, 2012, 2017], which discussed a violation of the correlation between upper atmosphere parameters and solar activity in solar cycles 18–23 (in particular, over the observatory Tory (52° N, 103° E)). The direct correlation weakened during strong La Niña events and solar minimum [Mikhalev et al., 2008]. The authors concluded that the variations in the parameters of the upper atmosphere may also be due to the variations in solar activity and fluctuations in the ocean — atmosphere sys-

tem. In this paper, we examine the ENSO effect on variations in zonal wind velocity, temperature, and geopotential height during El Niño and La Niña, using ERA-5 reanalysis data and data from the middle and upper atmosphere model up to altitudes of 100 km.

1. DATA

We have used the middle and upper atmosphere model (MUAM) to simulate the winter atmospheric circulation. MUAM is a three-dimensional nonlinear model of the general atmospheric circulation, implemented on a grid of 5.625° in longitude, 5° in latitude [Pogoreltsev et al., 2007]. A log-pressure height, $z = -H \ln(p/1000)$, is utilized as a vertical coordinate, where p is the pressure in hPa, H=7 km. The latest MUAM version involves parameterizing the effects of orographic gravity waves [Gavrilov, Koval, 2013]. In addition, we have employed climatic distributions of ozone and water vapor in the troposphere, taking into account longitude variations [Suvorova, Pogoreltsev, 2011]. MERRA data on convective precipitation has been used to specify ENSO conditions in MUAM. Heating rates were calculated by the empirical formula proposed in [Hong, Wang, 1980]. Using the Multivariate ENSO Index (MEI) as the base, we have selected years of ENSO positive and negative phases for which we have constructed the latent heat temperature composites and lower boundary conditions for January of these years. The heating rate distribution was approximated by a set of zonal harmonics with wave numbers m=1÷4 [Ermakova et al., 2019]. We have used ensemble calculations of 10 model implementations for the ENSO positive phase and 10 implementations for its negative phase.

The model calculations for January atmospheric conditions were compared with ERA-5 reanalysis data [Hersbach et al., 2020]. To assess the spatial structure of the atmospheric response to ENSO, we have plotted distributions of parameter differences (zonal wind velocity, air temperature, geopotential height between El Niño and La Niña phases). Table shows the El Niño and La Niña years used for the calculations. Note that the use of differences, rather than the parameter values themselves, makes it possible to take into account El Niño and La Niña effects at a time, yet it can distort the spatial structure of atmospheric responses both according to model calculations and according to climate archives. The atmospheric response to La Niña is similar to the response to El Niño with the opposite sign, but is still not identical both due to the differences in the spatial structure of temperature anomalies at the lower boundary of the atmosphere, and due to the differences in the properties of the troposphere and the middle atmosphere [Sobaeva et al., 2023]. Figures below confirm this point of view. Moreover, the calculations show that the differences have a more complex spatial structure than temperature anomalies separately during El Niño and La Niña, which hampers the comparison between reanalysis data and model calculations. To assess the statistical significance of the differences, we have calculated the reliability in a standard way, assuming that signal amplitude distributions (Student's t-test) are normal, and have plotted the distributions in the form of isolines on the constructed distributions of parameter differences.

As noted above, height levels in MUAM are represented in a log-pressure coordinate system in meters. Pressure in hectopascals is utilized as a vertical coordinate in the ERA-5 data. To analyze and compare the model and reanalysis data, we have taken levels of 15, 30, and 55 km according to MUAM and 100, 10, and 1 hPa according to ERA-5. For convenience, in what follows the heights will be given in kilometers.

1.1. Temperature

To assess the ENSO effect on the temperature of the middle atmosphere, we have plotted spatial distributions of air temperature differences between El Niño and La Niña ($\Delta T = \overline{T_{El}} - \overline{T_{La}}$) (Figure 1) according to reanalysis (*a–c*) and model (*d–f*) data. Maximum ΔT at ~15 km is seen to occur over the tropical Pacific Ocean, tropical Asia and Africa, and near the northern coast of North America. Note that at heights of the lower stratosphere, the spatial structures of ΔT according to reanalysis (±4 K) and model (from –5 to +7 K) data are similar, but ΔT according to the model is several degrees higher. The model does not reproduce temperature differences between tropical Asia and Africa. The reason is most likely to be an inaccurate setting of boundary conditions for El Niño and La Niña in the model. At 30 km, spatial distributions of ΔT are seen to differ, but the maximum signal from ENSO is observed near the North Pole in both

El Niño/La Niña in 1982–2022 [https://www.ncdc.noaa.gov/teleconnections/enso/sst]. We averaged the data from January 1 to January 31 over the years shown in the second row separately for El Niño and La Niña events.

	1982–2002														
El Niño	+2.2 °C			+1.7 °C			+1.6 °C					+2.4 °C			
	82	83		87	88		91	92	93	94	95	98			
La Niña		–1.1 °C			–1.9 °C					–1.0 °C			–1.7 °C		
		84	85	86	89	90				96	97		99	00	01	02

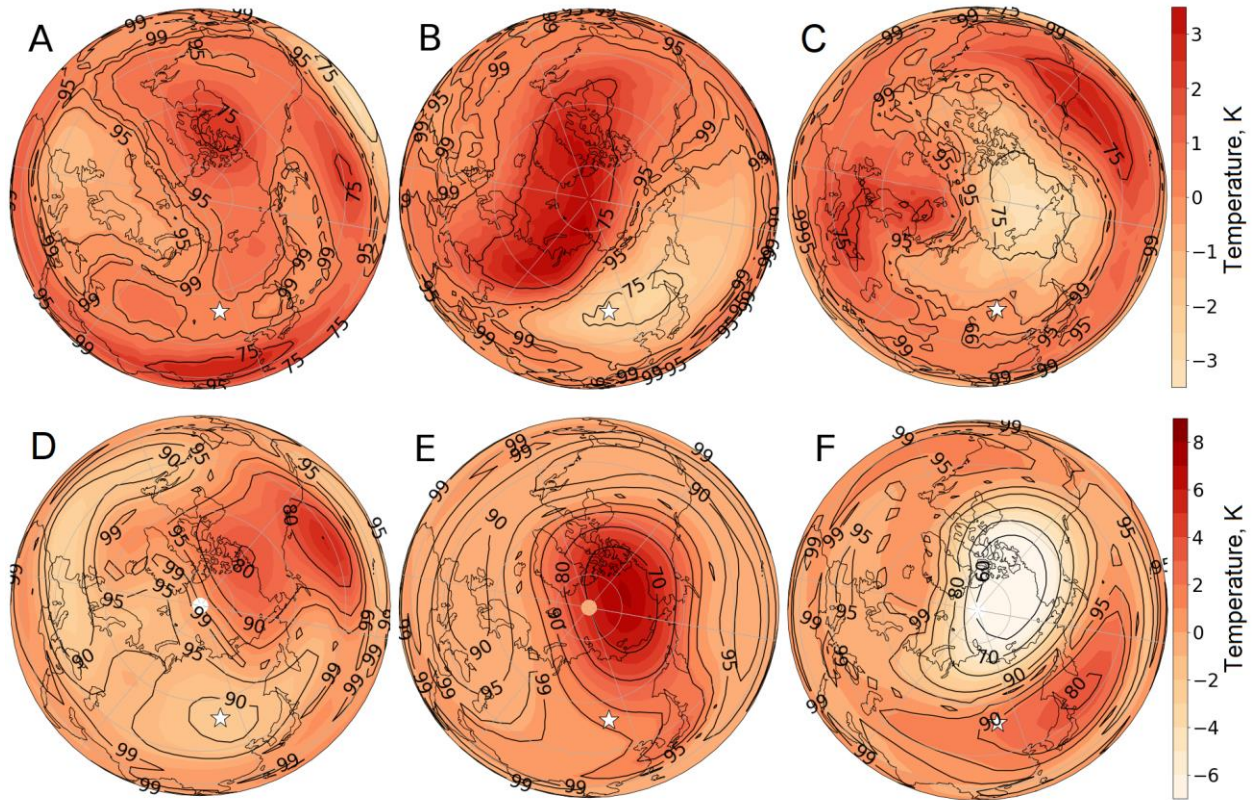|	2003–2022												
El Niño	+1.2 °C			+1.6 °C		+2.6 °C			0.8 °C				
	03	04	05	10		15	16		19	20			
La Niña		–1.6 °C			–1.6 °C			–0.9 °C			–1.3°C		
		06	08	09	11	12	13	14	17	18		21	22

A.N. Vyatkin, O.S. Zorkaltseva, V.I. Mordvinov

Figure 1. Spatial distribution of ΔT according to ERA5 (*a–c*) and MUAM (*d–f*) data at levels of 15, 30, 55 km respectively (fill); distribution of the statistical significance of ΔT according to Student's t-test (isolines). The asterisk in the panels indicates Irkutsk

model and reanalysis data. There are positive ΔT in the upper stratosphere at 55 km over Europe and the Atlantic, and negative ones over the north of Canada and the eastern Arctic Ocean. In the ERA-5 data, positive ΔT is visible over the Pacific Ocean, which is not reproduced by MUAM. Thus, the modeling and the reanalysis are generally consistent, at least in the middle and high latitudes, and show that during El Niño the polar vortex zone is warmer than during La Niña in the lower and middle stratosphere. In the upper stratosphere, on the contrary, at high latitudes the temperature is lower during El Niño. At low latitudes, the agreement between the observational data and the calculation results is worse, which is most likely due to an inappropriate setting of boundary conditions and a peculiarity of the analysis technique — the use of the El Niño — La Niña temperature difference instead of temperature anomalies in each individual case.

To analyze the ENSO effect on the atmosphere of Eastern Siberia in more detail, we have plotted height sections of the temperature difference (Figure 2) along 52.5° N (*a, c*) and 104° E (*b, d*). The greatest ΔT is seen to occur from 25 to 45 km above the Atlantic and North America to the north of 60° N. Above ~50 km, ΔT changes sign. Eastern Siberia is located near the border of positive and negative ΔT. Apparently, the border location of the region is the main reason for the differences in the estimated nature of the ENSO effect on the inland areas of Eurasia. In the middle stratosphere (see Figures 1, *b* and

2, *d*) over Siberia and the Far East, there is a range of negative ΔT that is not reproduced by the model, which is most likely a consequence of the ΔT anomalies in the upper low-latitude troposphere (see Figure 2, *d*), which are also absent in the model data.

The fact that the region of interest is located near the boundary of positive and negative values of mean temperature differences during El Niño and La Niña is probably responsible for the low reliability of the calculated differences since a relatively small spatial shift in the atmospheric response to ENSO can lead to significant anomalies or a change in the sign of the differences. This factor complements other fairly obvious reasons for the significant differences in the response of mean temperatures and other atmospheric parameters to changes in the ENSO indices. Firstly, this may be due to differences in the spatial structure of sea surface temperature (SST) and hence in the spatial structure of the atmospheric response during individual ENSO events. Secondly, SSW has a great impact on the mean zonal characteristics of the atmosphere. All SSW events vary in onset time, duration, and types. The total effect of SSW can lead to a wide spread of the average January atmospheric parameters. The listed factors relate largely to the reanalysis data. In model calculations, we can control some of the external factors, but even in the model the atmosphere remains unstable and long waves with an uncontrolled phase can arise and propagate in it, as well as SSW events can develop at arbitrary points in time.
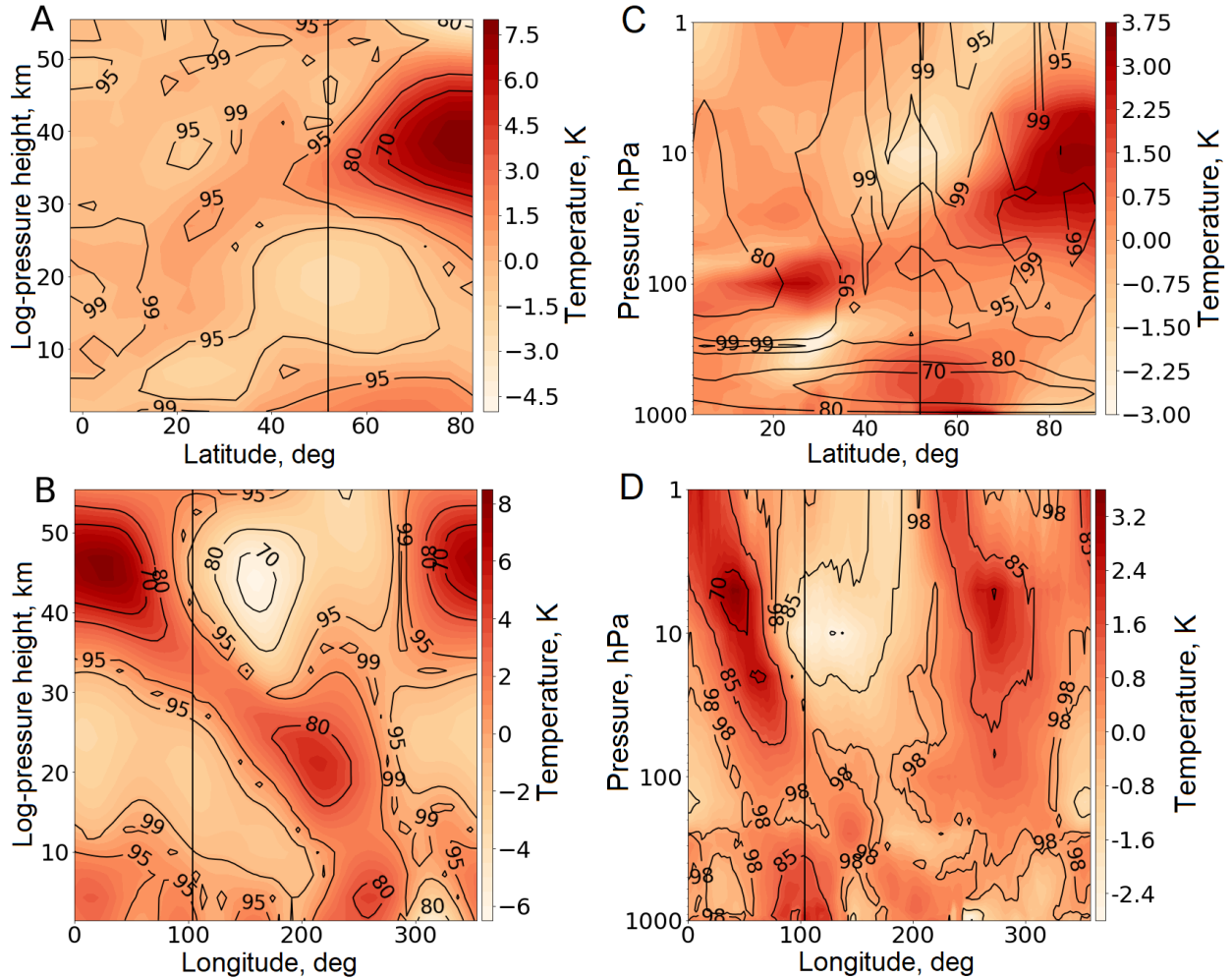
Figure 2. Vertical distribution of ΔT from the surface to 55 km according to MUAM (*a, b*) and ERA-5 (*c, d*) data. At the top is the distribution of ΔT along 104° E; at the bottom, along 52.5° N (fill); distribution of the statistical significance of ΔT by Student's t-test (isolines)

1.2. Zonal component of wind velocity

Spatial distributions of differences in the zonal component of wind velocity ΔU during El Niño and La Niña are illustrated in Figure 3. We can see that at all heights the spatial structures of ΔU according to MUAM and ERA-5 data are generally consistent, yet the model data overestimates ΔU approximately by a factor of two. At all heights, the quasi-wave structure of ΔU can be traced over the Pacific Ocean: at low latitudes, positive ΔU; at midlatitudes, negative; and to the north of 80° N, positive ones again. This confirms the conclusions of other authors about the wave mechanism of energy transfer during El Niño. However, Figures show quite a lot of differences, especially at low latitudes, the possible causes of which we have already discussed above.

If we consider ΔU in a vertical cross-section (Figure 4), there is an alternating structure at low latitudes, as derived from ERA-5 data, which is not reproduced so clearly by the model (panels *a, b*). Moreover, the alternating anomalies of ΔU over the Pacific Ocean at 30 and 55 km according to MUAM data (see Figure 3, *e, f*) turn out to be more extended in the latitudinal direction

than according to the reanalysis data, and reach Eastern Siberia, which is why we can see differences between ERA-5 and MUAM data on the vertical profiles (see Figure 4, *c, d*). The MUAM data exhibits a significant decrease in the zonal flow velocity at midlatitudes of the atmosphere during El Niño; the ERA-5 data shows a less pronounced decrease in the velocity. Despite the regional differences in ΔU, the general patterns of the signal from ENSO according to the model and reanalysis data are in good agreement.

Just as in the previous figures with ΔT (Figures 1, 2), the significance of the calculated differences is plotted on the velocity difference distribution maps. In general, the situation with the spread of differences according to both reanalysis data and calculations appears to be about the same as for the mean zonal temperature, or even worse, since the field of velocity differences is more variable in space than the fields of temperature difference and geopotential height difference (next Section). The differences in the spatial structure of the response from one event to another in the zonal velocity should therefore be more pronounced than in other parameters.
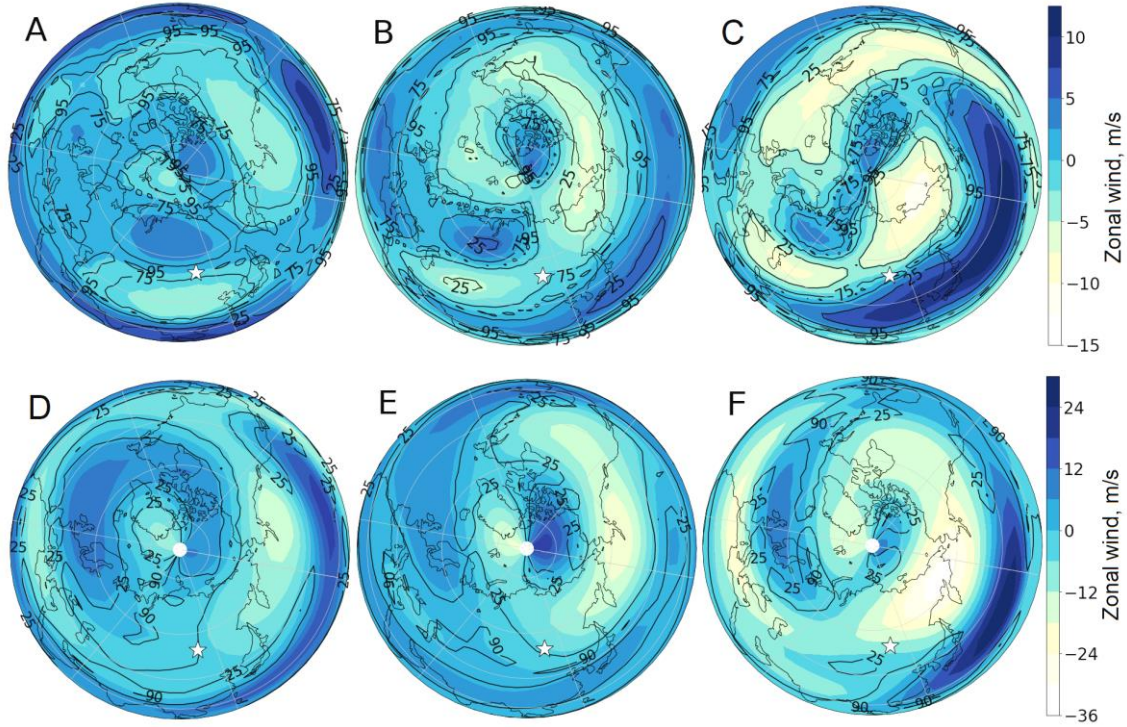
Figure 3. Spatial distribution of zonal wind anomalies of ΔU according to ERA5 (*a–c*) and MUAM (*d–f*) data at 15, 30, 55 km respectively (fill); distribution of statistical significance of ΔU according to Student's t-test (isolines). The asterisk in the panels indicates Irkutsk
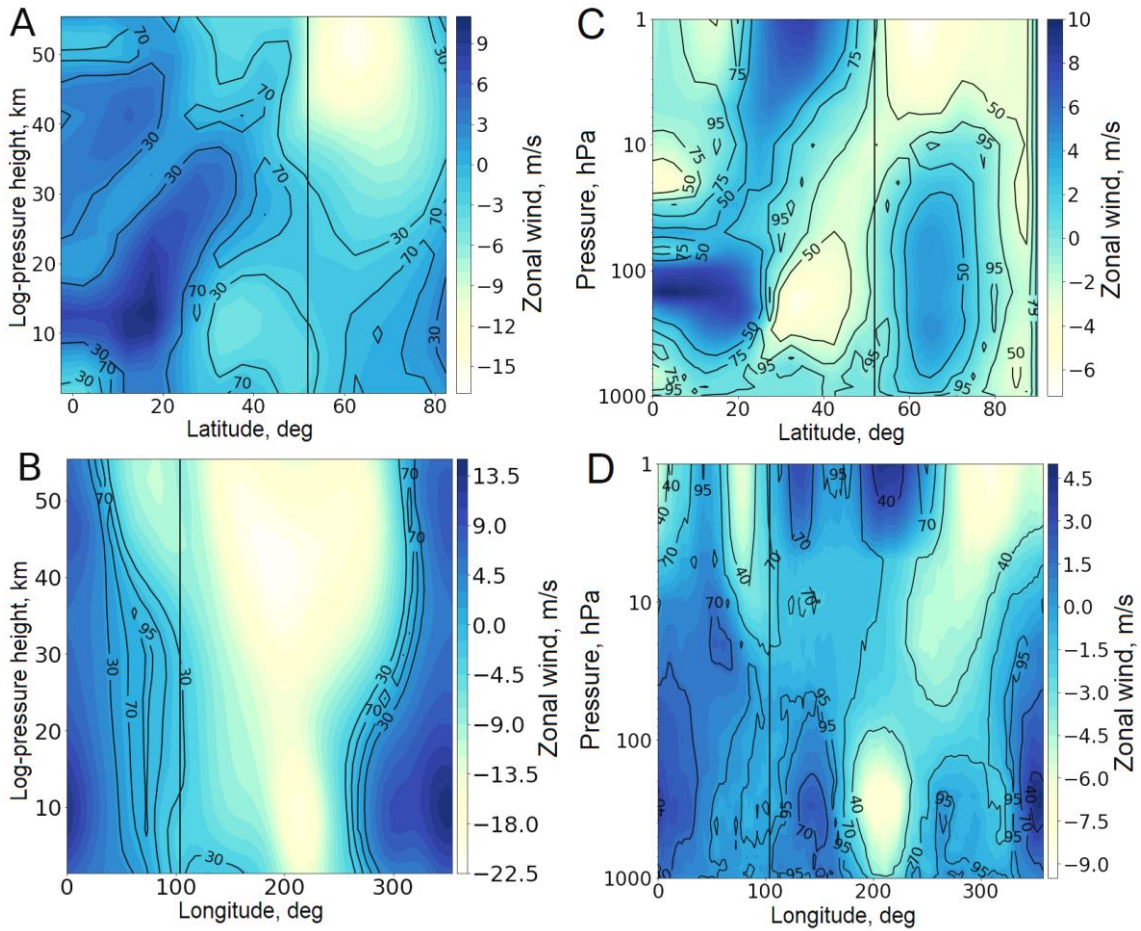

Figure 4. Vertical distribution of ΔU from surface to 55 km according to MUAM (*a*, *b*) and ERA-5 (*c*, *d*) data. At the top is the distribution of ΔU along 104° E; at the bottom, along 52.5° N (fill); distribution of statistical significance of ΔU according to Student's t-test (isolines)

1.3. Geopotential height

Distribution of geopotential height differences ΔP during El Niño and La Niña (Figure 5) shows that the maximum response is observed in the high-latitude upper stratosphere. Positive ΔP anomalies indicate that the stratospheric polar vortex during El Niño is weaker than during La Niña, which is consistent with the results obtained in [Garfinkel, Hartmann, 2008]. However, in the lower and middle stratosphere, the spatial pattern of ΔP according to ERA-5 data is more complex — there are two centers of positive and negative ΔP there. One positive center is located above Siberia. These differences can also be traced in vertical cross-sections along the latitude of Irkutsk (Figure 6, *a*, *c*). In the upper stratosphere, according to both MUAM and ERA-5, the ENSO effect on Eastern Siberia is insignificant.

The significance of the differences varies quite widely, but in general turns out to be quite high. Conspicuous is the similarity between the regions with a low level of significance and the regions with high levels of geopotential height differences. This indicates that the spread of values between events is more typical for regions with the greatest response to El Niño and La Niña. The spatial structure of the atmospheric response to El Niño and La Niña and the boundaries of alternating regions change to a lesser extent than the signal amplitude.

2. VERTICAL PROFILES OF ΔT, ΔU, ΔP TO 100 km OVER EASTERN SIBERIA

Analysis of the spatial pattern of the response of meteorological parameters to ENSO has generally shown a good agreement between MUAM and ERA-5 reanalysis data. Nonetheless, central Eurasia and Eastern Siberia are located on the periphery of the ENSO signal, so relatively small variations in the structure of the phenomenon can lead to variations in the upper atmosphere even with the same ENSO indices, as well as to differences in modeling results and observational data. To illustrate this conclusion, Figures 7, 8 show the vertical profiles of ΔT, ΔU, ΔP over points with coordinates 52.5°–57.5° N, 100°–110° E (Eastern Siberia) (see Figure 7) and 80°–85° N, 90°–95° W (Canadian Arctic Islands) (see Figure 8). The second point was chosen in the region of a strong response of the upper atmosphere meteorological parameters to ENSO. We can clearly see that there are significant differences in the response structure according to the simulation results and observations over Eastern Siberia up to changes in the response sign, as well as a good correspondence between the observational data and the calculation results over the Canadian Arctic Islands. This confirms our assumption.
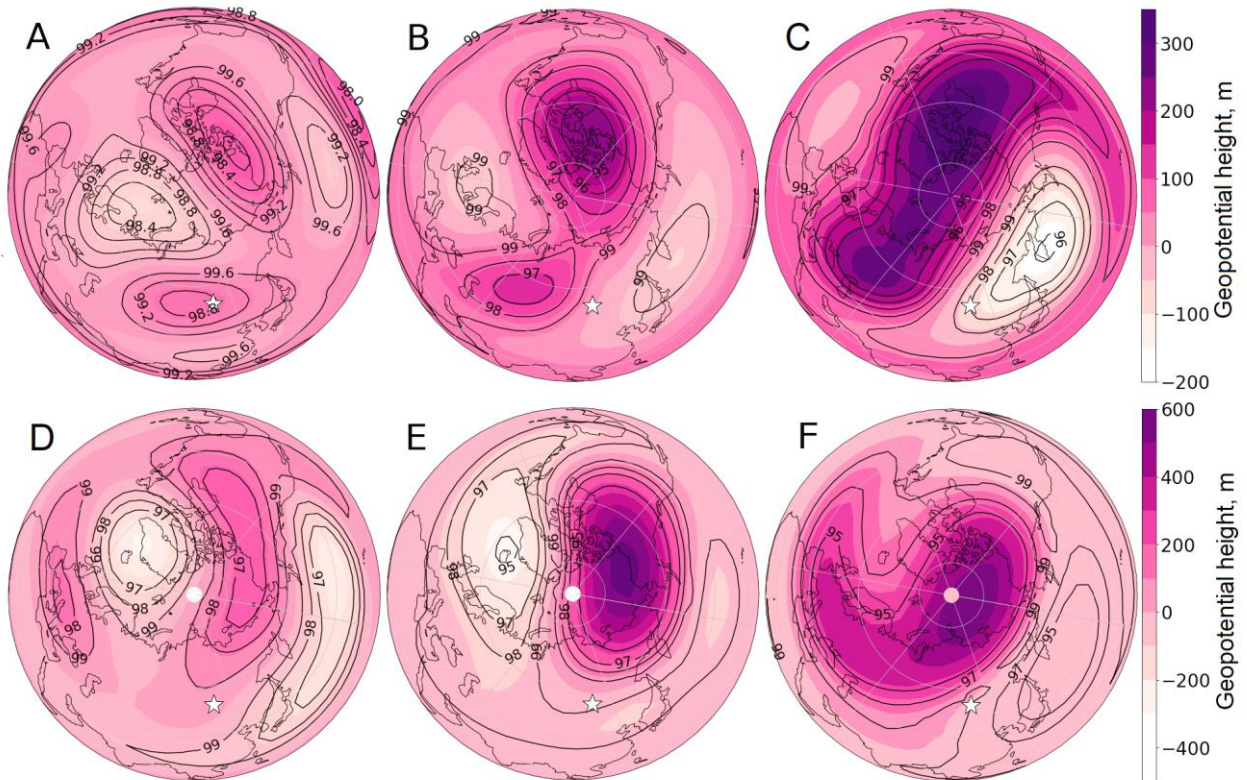

Figure 5. Spatial distribution of anomalies of geopotential heights of ΔP according to ERA-5 (*a–c*) and MUAM (*d–f*) data at 15, 30, and 55 km, respectively (fill); distribution of statistical significance of ΔP according to Student's t-test (isolines). The asterisk in the panels indicates Irkutsk
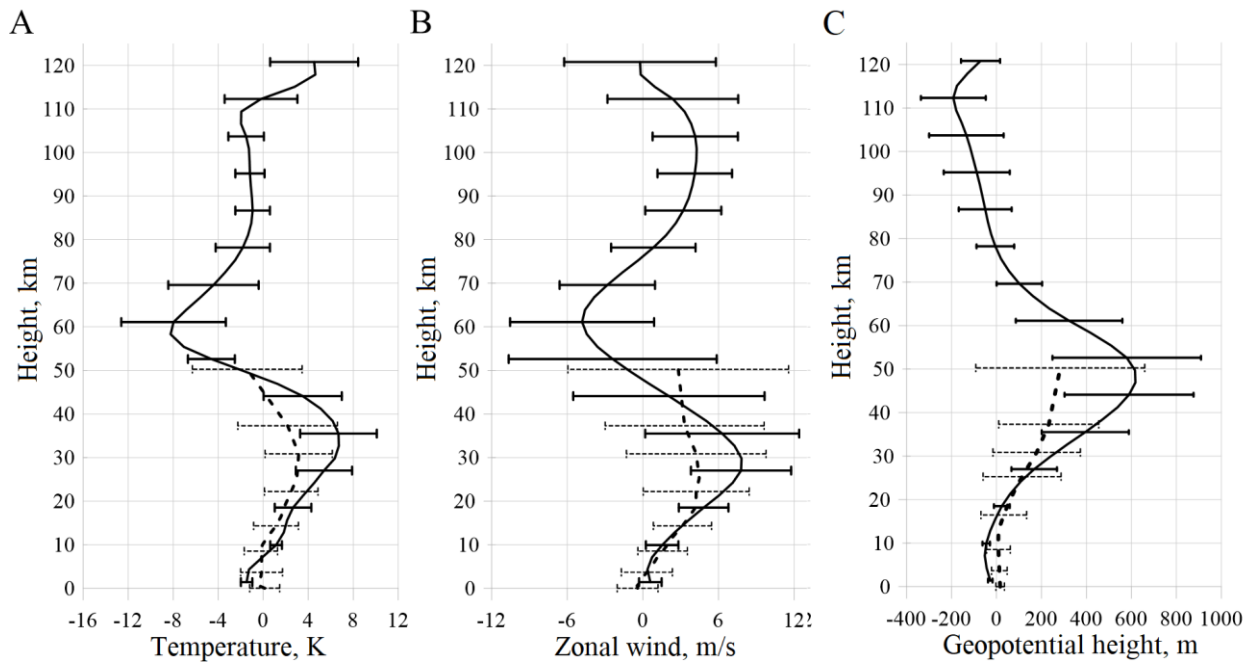
Figure 6. Vertical distribution of ΔP from surface to 55 km according to MUAM (*a*, *b*) and ERA-5 (*c*, *d*) data. At the top is the distribution of ΔP along 104° E; at the bottom, along 52.5° N (fill); distribution of statistical significance of ΔP according to Student's t-test (isolines)

Figure 7. Vertical profiles and rms deviations for ΔT (*a*), ΔU (*b*), ΔP (*c*) according to MUAM (solid line) and ERA (dashed line) data over Eastern Siberia

Figure 8. Vertical profiles and rms deviations for ΔT (*a*), ΔU (*b*), ΔP (*c*) according to MUAM (solid line) and ERA (dashed line) data over the territory of the Canadian Arctic Islands

Note also that root-mean-square (RMS) deviations were on average two times higher in Eastern Siberia than over the Canadian Arctic Islands according to both the model and the reanalysis. This suggests that over Eastern Siberia the atmospheric response to ENSO varies greatly from event to event, and so care should be exercised in using statistical methods to assess the response.

CONCLUSION

Despite a large number of studies into the El Niño Southern Oscillation, especially in the troposphere, there remained a lot of uncertainty in the behavior of the upper atmosphere parameters. The most difficult to interpret were variations in atmospheric parameters over the central regions of Eurasia, remote from the place of ENSO origin. In our study, we have compared reanalysis data with results of calculations made by specialized MUAM designed to reproduce the dynamics of the upper atmosphere. The simulation results confirmed the conclusions of other studies that pointed to the global nature of the response and the strong ENSO effect on the high-latitude polar atmosphere. Maximum response is observed in the high-latitude upper stratosphere. Positive pressure anomalies during El Niño indicate that the stratospheric polar vortex during El Niño is weaker than during La Niña according to both the model and reanalysis data. At the same time, the spatial structures of temperature differences according to reanalysis and modeling are similar, but ΔT according to the model is several degrees higher. Nonetheless, a maximum signal from ENSO is observed near the North Pole in both the model and reanalysis data. Thus, the model and the reanalysis, at least in the middle and high latitudes, are consistent in general and show that during El Niño the polar vortex region is warmer than during La Niña in the lower and middle stratosphere. In the upper stratosphere, on the contrary, the temperature is lower during El Nino at high lati-

tudes. At all heights there is a quasi-wave structure of zonal wind velocity differences during El Niño and La Niña over the Pacific Ocean. This confirms the conclusions of other authors about the wave mechanism of energy transfer during El Niño. According to both the model and reanalysis data, the inland areas fall into the border between the strong atmospheric response at low and high latitudes at the periphery of the main ENSO signal. In January, ENSO has the greatest impact on the polar middle atmosphere in the Northern Hemisphere. Over Eurasia and Eastern Siberia, the atmospheric response to ENSO proves to be weak or absent. In practice, this leads to considerable differences between estimated effects from one case of El Niño or La Niña to another and is probably the reason for the different conclusions about the manifestation of ENSO in the intracontinental regions.

REFERENCES

Domeisen D.I., Garfinkel C.I., Butler A.H. The teleconnection of El Nino Southern Oscillation to the stratosphere. *Rev. Geophys.* 2019, vol. 57, pp. 5–47. DOI: 10.1029/2018RG000596.

Ermakova T.S, Aniskina O.G., Statnaia I.A., Motsakov M.A., Pogoreltsev A.I. Simulation of the ENSO influence on the extratropical middle atmosphere. *Earth, Planets and Space.* 2019. DOI: 10.1186/s40623-019-0987-9.

Ermakova T.S., Koval A.V., Smyshlyaev S.P., Didenko K.A., Aniskina O.G., Savenkova E.N., Vinokurova E.V. Manifestations of Different El Niño Types in the Dynamics of the Extratropical Stratosphere. *Atmosphere.* 2022, vol. 13, no.12.2111. DOI: 10.3390/atmos13122111.

Garcia-Herrera R., Calvo N., Garcia R.R., Giorgetta M.A. Propagation of ENSO temperature signals into the middle atmosphere: A comparison of two general circulation models and ERA-40 reanalysis data. *J. Geophys. Res.* 2006, vol. 111, iss. D6. DOI: 10.1029/2005JD006061.

Garfinkel C.I., Hartmann D.L. Different ENSO teleconnections and their effects on the stratospheric polar vortex. *J. Geophys. Res.* 2008, vol. 113, iss. D18. DOI: 10.1029/2008JD009920.

Gavrilov N.M., Koval A.V. Parameterization of mesoscale stationary orographic wave impact for usage in numerical models of atmospheric dynamics. *Izvestiya Atmospheric and Oceanic Physics.* 2013, vol. 49, no. 3, pp. 271–278. (In Russian).

Hersbach H., Bell B., Berrisford P., Hirahara S., Horányi A., Muñoz-Sabater J., et al. The ERA5 global reanalysis. *Quarterly J. Royal Meteorological Society.* 2020, vol. 146, no. 730, pp. 1999–2049.

Hong S-S., Wang P-H. On the thermal excitation of atmospheric tides. *Bull. Geophys.* 1980, vol. 19, pp. 56–84.

Jacobi Ch., Kürschner D. A possible connection of midlatitude mesosphere/lower thermosphere zonal winds and the Southern Oscillation. *Phys. Chem. Earth.* 2002, vol. 27, pp. 571–577. DOI: 10.1016/S1474-7065(02)00039-6.

Jacobi Ch., Ermakova T., Mewes D., Pogoreltsev A.I. El Niño influence on the mesosphere/lower thermosphere circulation at midlatitudes as seen by a VHF meteor radar at Collm (51.3° N, 13° E). *Adv. Radio Sci.* 2017, vol. 15, pp. 199–206. DOI: 10.5194/ars-15-199-2017.

Li T., Calvo N., Yue J., Dou X., Russell III. J.M., Mlynczak M.G., She C.-Y., Xue X. Influence of El Niño-Southern Oscillation in the mesosphere. *Geophys. Res. Lett.* 2013, vol. 40, pp. 3292–3296. DOI: 10.1002/grl.50598.

Lu C., Liu Y., Liu C. Middle atmosphere response to ENSO events in Northern Hemisphere winter by the Whole Atmosphere Community Climate Model. *Atmosphere-Ocean.* 2011, vol. 49, iss. 2, pp. 95–111. DOI: 10.1080/07055900.2011.576451.

Lubis S.W., Matthes K., Omrani N.-E., Harnik N., Wahl S. Influence of the Quasi-Biennial Oscillation and Sea Surface Temperature Variability on Downward Wave Coupling in the Northern Hemisphere. *J. Atmos. Sci.* 2016, vol. 73, pp. 1943–1965. DOI: 10.1175/JAS-D-15-0072.1.

Mikhalev A.V. Some peculiarities of long-term variations of the Earth's upper atmosphere radiation in connection with changes in atmosphere–ocean climatic system. *Solar-Terr. Phys.* 2012, iss. 21, pp. 62–66. (In Russian).

Mikhalev A.V. The [OI] 557.7 nm airglow emission during El Niño/La Niña extreme events in solar cycles 23–24. *Atmospheric and ocean optics.* 2017, no. 11, pp. 986–989. DOI: 10.15372/AOO20171112. (In Russian).

Mikhalev A.V., Stoeva P., Medvedeva I.V., Benev B., Medvedev A.V. Behavior of the atomic oxygen 557.7 nm atmospheric emission in the solar cycle 23. *Adv. Space Res.* 2008, vol. 41, iss. 4, pp. 655–659. DOI: 10.1016/j.asr.2007.07.017.

Pogoreltsev A.I., Vlasov A.A., Frцhlich K., Jacobi Ch. Planetary waves in coupling the lower and upper atmosphere. *J. Atmos. Solar-Terr. Phys.* 2007, vol. 69, pp. 2083–2101.

Richter J.H., Matthes K., Calvo N., Gray L.J. Influence of the quasi-biennial oscillation and El Niño–Southern Oscillation on the frequency of sudden stratospheric warmings. *J. Geophys. Res.* 2011, vol. 116, D20111. DOI: 10.1029/2011JD015757.

Sobaeva D., Zyulyaeva Y., Gulev S. ENSO and PDO Effect on Stratospheric Dynamics in IscaNumerical Experiments. *Atmosphere.* 2023, vol. 14, iss. 3, 459 p. DOI: 10.3390/atmos14030459.

Suvorova E.V., Pogoreltsev A.I. Modeling of nonmigrating tides in the middle atmosphere. *Geomagnetism and Aeronomy.* 2011, vol. 51, no 1, pp. 107–118. (In Russian).

Taguchi M., Hartmann D.L. Increased occurrence of stratospheric sudden warmings during El-Niño as simulated by WACCM. *Journal of Climate.* 2006, vol. 19, iss. 3. P. 324–332. DOI: 10.1175/jcli3655.1.

Wang X.Y., Zhu J., Chang C.H., Johnson N.C., Liu H., Li Y., et al. Underestimated responses of Walker circulation to ENSO-related SST anomaly in atmospheric and coupled models. *Geophys. Lett.* 2021, vol. 8, no. 17. DOI: 10.1186/s40562-021-00186-8.

URL: https://www.ncdc.noaa.gov/teleconnections/enso/sst (accessed January 30, 2023).

How to cite this article
Vyatkin A.N., Zorkaltseva O.S., Mordvinov V.I. Influence of El Niño on parameters of the middle and upper atmosphere over Eastern Siberia according to reanalysis and model data in winter. *Solar-Terrestrial Physics*. 2024. Vol. 10. Iss. 1. P. 40–48. DOI: 10.12737/stp-101202406.